JCTC Journal of Chemical Theory and Computation

Article

pubs.acs.org/JCTC

Importance and Nature of Short-Range Excitonic Interactions in Light Harvesting Complexes and Organic Semiconductors

Rocco P. Fornari,[†] Patrick Rowe,[§,†] Daniele Padula,[†] and Alessandro Troisi*[,†,‡]

[†]Department of Chemistry, University of Warwick, Coventry CV4 7AL, United Kingdom

[‡]Department of Chemistry, University of Liverpool, Liverpool L69 7ZD, United Kingdom

Supporting Information

ABSTRACT: The singlet excitonic coupling between many pairs of chromophores is evaluated in three different light harvesting complexes (LHCs) and two organic semiconductors (amorphous and crystalline). This large database of structures is used to assess the relative importance of short-range (exchange, overlap, orbital) and long-range (Coulombic) excitonic coupling. We find that Mulliken atomic transition charges can introduce systematic errors in the Coulombic coupling and that the dipole−dipole interaction fails to capture the true Coulombic coupling even at intermolecular distances of up to 50 Å. The non-Coulombic short-range contribution to the excitonic coupling is found to represent up to ∼70% of the total value for molecules in close contact, while, as expected, it is found to be negligible for dimers not in close contact. For the face-to-face dimers considered here, the sign of the short-range interaction is found to correlate with the sign of the Coulombic coupling, i.e. reinforcing it when it is already strong. We conclude that for molecules in van der Waals contact the inclusion of short-range effects is essential for a quantitative description of the exciton dynamics.

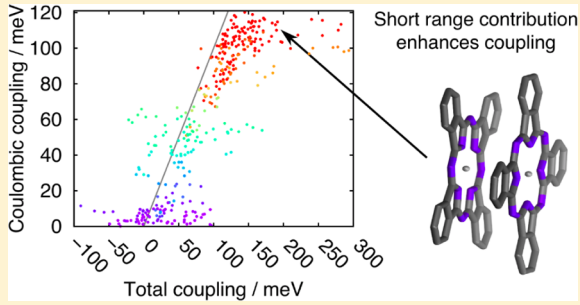

INTRODUCTION

The excitonic coupling between localized Frenkel excitons determines the dynamics of electronic energy transfer in a variety of molecular systems, including biological light harvesting complexes[1,2] and organic semiconductors.[3,4] For the study of the quantum mechanical evolution of excited states it has become commonplace to evaluate the excitonic coupling for a large number of structures, e.g. those deriving from a molecular dynamics simulation[5−13] or representing the interaction between chromophores in an amorphous system.[14−20] To perform these large scale simulations efficiently, to rationalize the observed properties, and to design new materials it is important to identify the main components of the excitonic coupling and assess their relative importance.

The excitonic coupling is conventionally separated into a Coulombic contribution, which dominates interactions at large distances and a number of short-range contributions, which are important for molecules in close contact.[2,21] The Coulombic coupling is[22−24]

$$J^{C} = \int\int \frac{\rho^{a}(\mathbf{r}_i)\cdot\rho^{b}(\mathbf{r}_j)}{|\mathbf{r}_i - \mathbf{r}_j|} d\mathbf{r}_i d\mathbf{r}_j \cong \sum_{i,j}^{N_{grid}} \frac{\rho_i^{a}\cdot\rho_j^{b}}{|\mathbf{r}_i - \mathbf{r}_j|} \quad (1)$$

where $\rho^{a(b)}(\mathbf{r})$ is the value of the transition density of the localized Frenkel exciton a (b). In practice, the integral in eq 1 is evaluated numerically as a summation over a grid of points $\{\mathbf{r}_i\}$ commonly called transition density cube (TDC),[25] with $\rho_i^{a(b)} = \rho^{a(b)}(\mathbf{r}_i)$.

Evaluating J^{C} from TDCs can be computationally demanding due to the large number of grid points (∼10^6 for the molecules considered here) needed to reach convergence. For this reason, it is often assumed that approximations based on coarser representations of the transition density are appropriate. When the distance between molecules is comparable to the molecular sizes, one can discretize the transition density on atom centered charges[25,26] (atomic transition charges, ATC), while for very distant pairs the dipole−dipole approximation[27] is often used.

The nature and relative importance of the different contributions to the excitonic coupling were thoroughly analyzed more than 20 years ago by Harcourt, Scholes, and Ghiggino in a series of studies.[28−30] By considering the interaction between Frenkel and charge-transfer excited configurations,[28] they identified the dominant non-Coulombic short-range contributions, both depending on intermolecular orbital overlap: a penetration interaction, which generally reinforces the Coulombic term,[29] and the Dexter exchange interaction, which opposes it but is of much smaller magnitude.[30] The total excitonic coupling, which captures the global effect of Coulombic and short-range contributions, can be computed relatively easily − albeit at a higher computational cost − by using one of the available diabatization techniques based on various molecular properties.[21,31−34] In these approaches, the adiabatic electronic Hamiltonian of the system is transformed into a diabatic Hamiltonian where the off-

Received: March 27, 2017
Published: June 26, 2017

DOI: 10.1021/acs.jctc.7b00328
J. Chem. Theory Comput. 2017, 13, 3754−3763

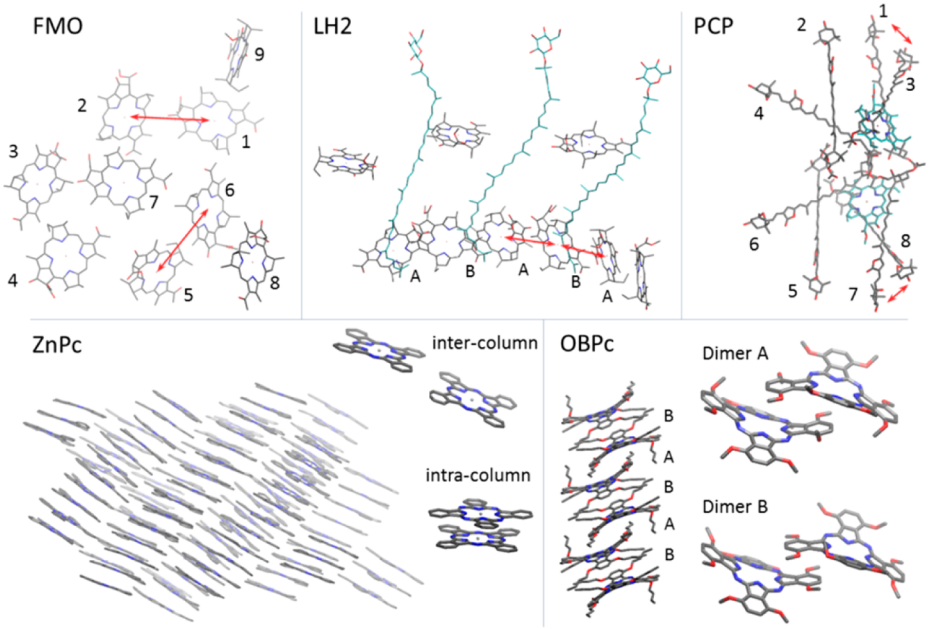

Figure 1. Structures of the LHCs (top) and molecular materials (bottom) considered. Hydrogens are omitted in all structures. Top: Only the chromophores are shown. One third of the LH2 complex is considered. The phytyl chain of BChlA and ChlA is replaced by methyl. The red arrows indicate the pairs with the strongest short-range interactions. Bottom left: Disordered sample of 90 ZnPc molecules and examples of inter- and intracolumn dimers. Bottom right: stacking of the molecules in the OBPc crystal and details of the two dimers (with butoxy replaced by methoxy). Numeric labels indicate chromophores, while letters indicate equivalent pairs. The structure figures were generated with VMD.[57]

diagonal elements are the couplings between diabatic excited states. Although the different short-range contributions to the couplings cannot be distinguished when obtained from a diabatization, the non-Coulombic short-range interaction can be evaluated indirectly as the difference between the total coupling and the purely Coulombic coupling.

For a number of problems in the fields of biophysics and materials science it has become particularly important to be able to understand and quantify the effect of short-range interactions. In organic semiconductors, where the most important couplings are between molecules in contact, it is important to know whether the dominant interaction is still Coulombic (i.e., computable from eq 1), in which case it can still be treated by approximate representations of the transition density like ATC or dipole−dipole, or if the short-range component must also be included. This is a crucial question since the excitonic couplings determine the static and dynamic properties of molecular aggregates. The regime of exciton transport (coherent or incoherent) is determined by the relative strength of the excitonic coupling and the exciton−phonon coupling.[35−37] Furthermore, short-range interactions at finite temperature cause strong fluctuations in the excitonic coupling[3,13,36] which in some instances can influence or limit the energy transfer dynamics.[37−39] In photosynthesis, light absorption and efficient transport of the excitation energy are achieved by clusters of chromophores in proteins commonly called light harvesting complexes (LHCs).[2] Generally, the majority of chromophore pairs are sufficiently distant that their interaction is reasonably well described by expressions like (1). This has been shown to be true, for example, for most pairs in the well-studied FMO protein.[8] On the other hand, some LHCs such as LH2 contain chromophore pairs for which the intermolecular separation is small enough that short-range interactions may play an important role.[40] A highly debated point in the literature is the role of quantum mechanical coherence in the evolution of excited states in LHCs.[41−43] Any fluctuation of the excitonic couplings due to short-range interactions coupled to thermal motion is expected to decrease the coherence and affect the exciton dynamics.[39,44,45]

The aim of this paper is to evaluate the excitonic coupling between pairs of chromophores in three different LHCs and in two organic semiconductors (one amorphous and one crystalline), to achieve a broader understanding of the importance of short-range interactions valid for most of the problems under current consideration. This large database of structures is used to assess the role of short-range interactions with respect to the Coulombic one. The results will be also used to establish criteria for using approximate methods to evaluate the Coulombic interaction.

Systems Investigated. Among the astounding variety of LHCs that have been discovered, we have selected a few with the intent of covering a broad range of different chromophore arrangements: the Fenna-Matthews-Olson Protein (FMO) from *Chlorobium tepidum*,[46] the Light Harvesting II Protein (LH2) from *Rhodopseudomonas acidophila*[47], and the Peridinin Chlorophyll Protein (PCP) from *Amphidinium carterae*.[48] The FMO protein has become the model system for much research into exciton transport in LHCs since the initial report of coherent energy transfer.[41,49] Comprising of three identical subunits containing 8 bacteriochlorophyll-a (BChlA) chromophores each, FMO is relatively simple from a chemical perspective but is topologically complex, with no symmetry to the spatial arrangement of chromophores in space within a monomeric unit. LH2 is of great interest for the opposite reason: it is comprised of both BChlA and rhodopin glucoside (carotenoid) chromophores arranged in a C_9 symmetric structure giving rise to very peculiar effects such as spectral shifts and exciton delocalization[50] which may affect the coherent evolution of excitons.[23,40,42,51] We include PCP in our study as a representative LHC containing two different

DOI: 10.1021/acs.jctc.7b00328
J. Chem. Theory Comput. 2017, 13, 3754−3763

types of chromophores: two pseudo-2-fold symmetric sets of peridinin chromophores (carotenoids) and a pair of chlorophyll-a (ChlA) chromophores.[48,52] The arrangement of chromophores in these structures is illustrated in Figure 1.

To illustrate the role of short-range contributions to excitonic coupling in molecular materials, we have considered two examples with different morphologies, an ordered crystal (with dynamic disorder) and a partially disordered molecular solid. In both cases phthalocyanines have been chosen as they are widely studied and well performing semiconductors and because of their structural and spectroscopic similarity to natural chlorophylls. The ordered crystal is taken from a previous study by some of us,[36] where we investigated the effect of thermal fluctuations of the couplings on exciton dynamics in a molecular crystal of the metal-free octabutoxyphthalocyanine (OBPc), for which experimental evidence of exciton delocalization was previously reported.[53] The couplings in the two closely packed dimers of OBPc (see Figure 1) were evaluated for 250 snapshots separated by 50 fs along a molecular dynamics (MD). The data obtained in ref 36 are analyzed here with the purpose of characterizing and quantifying the role of the short-range component in the presence of thermal fluctuations. Disordered phases in organic semiconductors are of great interest as they make up a significant fraction of polycrystalline thin films, not to mention amorphous films. While the morphology of the crystalline phase is usually well characterized, this is not the case for the disordered regions, which are believed to be of crucial importance for charge and exciton transport as they connect crystalline regions.[54−56] To provide a plausible example of a partially disordered structure we have simulated the rapid thermal annealing from high temperature of the well-studied zinc phthalocyanine (ZnPc). The resulting solid, shown in Figure 1, is a sample of the noncrystalline phase where the molecules are preferentially stacked in columns with $\pi-\pi$ intermolecular distances in the 3.0−3.8 Å range. There is disorder both in the intracolumn rotational angles and in the tilt angles of adjacent columns, making this an interesting and statistically varied example for the comparison of long- and short-range excitonic interactions.

METHODS

The structures of the LHCs were obtained from the Protein Data Bank entries 3BSD[58] (FMO), 1NKZ[59] (LH2), and 1PPR[48] (PCP). All pairs of identical chromophores (*homodimers*) were considered, for which the role of charge transfer states and the effect of the relative alignment of excitation energy levels on the couplings can be neglected. This is not the case for *heterodimers* (i.e., chlorophyll-carotenoid), which were therefore excluded from this study. In FMO we have considered the 8 BChlA belonging to one of the subunits and, due to its proximity, one BChlA from the neighboring subunit. In LH2 we have considered all homodimers within one-third of the complex as shown in Figure 1, thereby avoiding the calculation of the weaker couplings. The phytyl chain of BChlA and ChlA was substituted with a methyl group since its effects on the excited state properties are not large enough to justify the additional computational cost of including it.[60] A plausible structure of the disordered phase of zinc phthalocyanine (ZnPc) was obtained from a molecular dynamics simulation performed with the GROMACS 5.0.5 software[61] using a force field parametrized for ZnPc.[62] A sample of 90 molecules starting from the experimental crystalline phase[63] was first equilibrated at 300 K (for 5 ns), then heated (over 5 ns), and equilibrated at 700 K (for 30 ns) under NVT conditions using a Nose-Hoover thermostat. Then it was repeatedly kept at 700 K for 10 ns and quenched to 300 K (over 5 ns) under NPT conditions using a Berendsen barostat obtaining after 6 such annealing cycles (and 204 ns total simulation time) a partially disordered phase stable at 300 K consisting of closely spaced columns. From the final snapshot at 300 K (shown in Figure 1) two sets of molecular pair configurations were extracted. The *intracolumn dimers* are defined as those where the distance between the centers of mass is less than 6 Å, and the *intercolumn dimers* are those where this distance is between 6 and 15 Å. The dimers where the molecules are within 15 Å but they are in the same column (i.e., they are second or third neighbors) are not considered. In summary, our data set consists of all homodimers from the LHCs, 90 intracolumn dimers and 10 intercolumn dimers from the ZnPc sample, and 250 MD snapshots for each dimer of OBPc.

Since we are more interested in comparing long- and short-range interactions in a large set of structures, rather than in the absolute accuracy of the couplings, it is desirable to exclude from our analysis the uncertainties in the experimental data (for the LHCs) and the uncertainties in the MD force field (for ZnPc). Therefore, all couplings (excluding OBPc) were computed using the same rigid molecular geometry, superposed on the original geometry with a root-mean-square distance minimization procedure using the *superpose* program included in TINKER 7.1.[64] For the LHCs the rigid geometry was obtained by optimizing the chromophore in vacuum at the LC-ωPBE/6-31G** level. For ZnPc, the experimental crystal structure[63] was taken as the rigid geometry. The singlet excited states of all molecules and dimers were computed with TDDFT at the LC-ωPBE/6-31G** level of theory (3-21G for OBPc) using the NWChem 6.6 software.[65] This particular long-range corrected density functional[66] with the parameter $\omega = 0.3a_0^{-1}$ was chosen as it was shown to correctly describe both localized and charge transfer excitations.[67] The effect of this choice was assessed by comparing the results with those obtained from two other range separated density functionals (LC-PBE and CAM-B3LYP) in a subset of dimers (*vide infra*). In most of the molecules considered, the lowest singlet excited states S_1 and S_2 were found to be relatively close in energy (ΔE_{12} = 0.5 eV in BChlA, 0.6 eV in ChlA, 0.8 eV in rhodopin, 0.02 eV in ZnPc, and 0.03 eV in OBPc), while S_3 was found to be higher (ΔE_{23} = 0.6−1.5 eV). Considering that the laser pulses used to excite the system in pump−probe experiments usually have a duration of 10−50 fs,[68] resulting in an excitation bandwidth of 0.08−0.4 eV, it seems likely that S_2 plays an important role in the ultrafast dynamics of the lowest excitons in these systems,[69,70] and it may influence the coupling between S_1 at close separations.[60] The importance of considering S_2 has been recognized for phthalocyanines[5] and porphyrins[71] although often only S_1 of BChlA is considered in studies of excitons in FMO[8] and LH2.[9] Therefore, with the exception of peridinin (where ΔE_{12} = 1.1 eV and ΔE_{23} = 0.3 eV), all intermolecular excitonic couplings J_{11}, J_{22}, J_{12}, and J_{21} were considered.

The Coulombic couplings were evaluated from eq 1 using the TDCs obtained from the TDDFT calculation. In order to avoid discontinuities due to grid points at short distances, which may occur for interpenetrating transition densities, we introduced at each volume element a Gaussian distribution of the charge density as in eqs 2 and 3 of ref 72. We verified that the results were converged with respect to the chosen grid size

DOI: 10.1021/acs.jctc.7b00328
J. Chem. Theory Comput. 2017, 13, 3754−3763

of 0.2 Å. The dielectric effect of the different mediums (protein, molecular solid) was neglected by setting the relative permittivity (dielectric constant) to 1, as the aim was to compare the relative importance of short- and long-range interactions, rather than the effect of the environment on these. As suggested in the literature, the effect of the environment could be taken into account by scaling the Coulombic coupling by an effective screening factor[73−76] derived from explicit or approximate inclusion of the polarizability of the protein or by the optical dielectric constant of the bulk material.[26] However, the dielectric is likely to play a more complex role as it can also change the excitation energies and transition dipole moments.[77] The overall effect of the dielectric can be approximated as a simple scaling factor of the coupling in the 0.5−0.9 range[26,74,78] in the Coulombic regime and as a negligible or very small strengthening of the short-range interactions.[34] Therefore, the dielectric is expected not to affect our qualitative conclusions, and its inclusion is beyond the scope of this work.

The total excitonic couplings between the localized Frenkel excitons S_1 and S_2 were computed for each molecular pair (dimer) using the diabatization procedure described in ref 34. The basic assumption of diabatization schemes is that the coupling between diabatic states can be obtained from the adiabatic states of the system by using a suitable molecular property to find the best adiabatic-to-diabatic transformation matrix $\mathbf{C}$. In our case $\mathbf{C}$ is obtained as the matrix which makes the ATCs of the diabatic excitations as similar as possible to the ATCs of reference states, chosen to be the excitations localized on the two molecules. This amounts to a linear algebra problem known as the orthogonal Procrustes problem, whose solution is explained in detail in ref 34. The (diagonal) adiabatic Hamiltonian $\mathbf{H}^A$, whose elements are the excitation energies of the dimer, is then transformed (diabatized) obtaining a diabatic matrix $\mathbf{H}^D = \mathbf{C}\mathbf{H}^A\mathbf{C}^T$ where $\mathbf{C}^T$ is the transpose of $\mathbf{C}$. The diagonal elements of $\mathbf{H}^D$ are the diabatic energies, and the off-diagonal elements are the intermolecular couplings J_{11}, J_{22}, J_{12}, and J_{21} (the intramolecular couplings are negligible due to orthogonality of $\boldsymbol{\mu}_1$ and $\boldsymbol{\mu}_2$ in the chlorophylls and phthalocyanines). The ATCs were computed from a transition density Mulliken population analysis[34,79] taking into account the CI vectors obtained from the TDDFT calculations of the single molecules and dimers.

RESULTS

The importance of short-range excitonic interactions was evaluated by comparing the Coulombic coupling and the total coupling for all molecular pairs at long and short intermolecular distances. It is customary to describe the total excitonic coupling $J^{TOT} = J^C + J^{short}$ as the sum of a Coulombic term, prevalent at intermediate to long distances, and a short-range contribution.[2,21] The sign of the excitonic coupling is determined by the signs of the wave functions in the basis set used for the excited state energy calculation. Since the transition densities of the localized excitations are used both for computing J^C and as reference states for obtaining J^{TOT}, their signs are guaranteed to be consistent. In order to have a consistent value of J^{short} and understand if it is strengthening or weakening J^{TOT} with respect to J^C, we arbitrarily choose the sign of the wave function to make J^C positive and report J^{TOT} with a consistent sign, i.e. with the same sign of the wave function.

Before comparing the couplings computed with different methods, it is essential to quantify their associated uncertainties and inaccuracies. Relative differences much smaller than these deviations will not form a good basis for quantitative predictions.

Systematic Errors in the Evaluation of the Coulombic Coupling. In this section we discuss a number of systematic errors that can affect the evaluation of the Coulombic coupling and that, consequently, may influence the assessment of the importance of short-range interactions. We start by reporting on the variability of the Coulombic excitonic couplings due to the use of different density functionals in all 36 BChlA dimers from FMO and in 20 ZnPc dimers (10 intracolumn and 10 intercolumn). We report deviations between the properties obtained from two other range-separated functionals (LC-PBE and CAM-B3LYP) with respect to the functional chosen for this work (LC-ωPBE). For the excited states of BChlA we found variations on $|\boldsymbol{\mu}_1|$ and $|\boldsymbol{\mu}_2|$ of 0.80% and −0.31% (LC-PBE), 2.4% and −3.6% (CAM-B3LYP). For ZnPc we found smaller variations of −0.29% and −0.25% (LC-PBE), 0.019% and 0.19% (CAM-B3LYP). For the Coulombic couplings J^C (from TDCs) we found RMS deviations (normalized by $\langle J^C_{LC\text{-}\omega PBE}\rangle$) of 6.4% (LC-PBE) and 12% (CAM-B3LYP) for BChlA and 2.2% (LC-PBE) and 3.8% (CAM-B3LYP) for ZnPc. These variations represent a first estimate of the uncertainty on J^C and will be taken into account when discussing the relative difference between J^{TOT} and J^C.

Next, it is necessary to evaluate the accuracy of computing J^C using approximate representations of the transition density (ATC and point dipole) compared with the full coupling from TDCs (eq 1). A preliminary examination found that in the roughly disc-shaped chlorophylls and phthalocyanines, the ATCs obtained from Mulliken population analysis overestimate by about 3% the norm of the transition dipole moment $\boldsymbol{\mu}$ with respect to the evaluation from the full TDDFT wave function, while this error is, expectedly, lower than 0.5% when the transition density is described by a transition density cube (TDC). The error is even more striking in the carotenoids examined (rhodopin glucoside in LH2 and peridinin in PCP) where the ATCs overestimate the norm of $\boldsymbol{\mu}$ by up to 20% as they fail to capture the transition density in the regions further away from the atoms, an effect amplified by the elongated shape and the large basis set. The TDCs are much more accurate, giving errors of 0.13% (rhodopin) and 0.05% (peridinin). When the ATCs are rescaled to reproduce the TDDFT transition dipole moment, the root-mean-square relative error between the Coulombic couplings obtained from ATCs compared to TDCs is reduced from 69% to 10% for peridinin. ATCs obtained by fitting to the electrostatic potential (the TrEsp method,[60] not considered in this study) have also been shown to represent the transition density of chlorophylls with accuracy comparable to TDCs.[80] In summary, we observe that in some cases, such as elongated molecules, the Mulliken ATCs do not describe the transition density with sufficient accuracy. Therefore, for the purpose of evaluating the short-range contributions with high accuracy, the Coulombic couplings J^C are computed from TDCs using eq 1 in the remainder of this paper.

The behavior of the different methods in the intermediate to long-range was then investigated by building a symmetric model dimer of two BChlA molecules arranged face-to-face (with an inversion point) and computing the couplings as a function of the distance between the centers of mass in the range 6−50 Å, measured along the vector normal to the molecular plane. First, we assessed the difference between the

DOI: 10.1021/acs.jctc.7b00328
J. Chem. Theory Comput. 2017, 13, 3754−3763

couplings computed using the dipole−dipole approximation and TDCs by computing $J^{C}_{dip\text{-}dip}/J^{C}_{TDC}$ as a function of distance and fitting the data with the following polynomial function of the distance d obtained from the ratio between the dipole−dipole term $U_{dip-dip}$ and the multipole term (up to hexadecapoles) $U_{multipole}$ of the electrostatic interaction:

$$\frac{U_{dip\text{-}dip}}{U_{multipole}}(d) = (1 + c_1 \cdot d^{-1} + c_2 \cdot d^{-2} + c_3 \cdot d^{-3} + c_4 \cdot d^{-4} + c_5 \cdot d^{-5} + c_6 \cdot d^{-6})^{-1} \quad (2)$$

The results, reported in the top panel of Figure 2, show that the multipole (higher than dipole) terms, captured by the

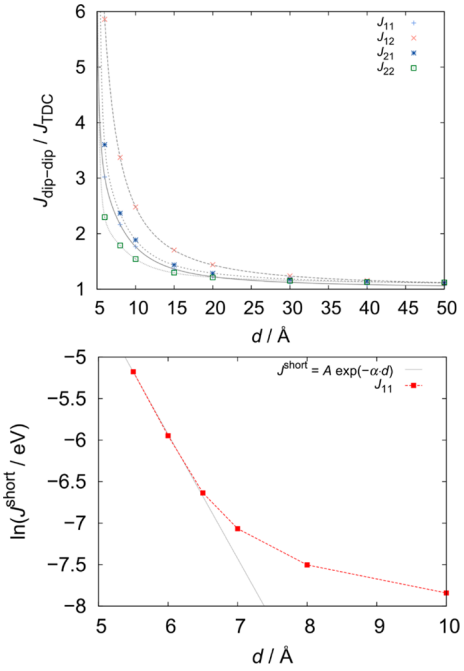

Figure 2. Ratio between dipole−dipole[27] and TDC (eq 1) Coulombic couplings as a function of distance. The gray lines are obtained from fitting the data points with eq 2. Bottom: Distance dependence of the short-range component. The solid line is obtained by fitting the data to the equation shown in the figure between 5.5 and 6.5 Å. The fitting parameters are A = 21.4 eV and α = 1.50.

TDCs, make up a large fraction (67% at 6 Å and 6% at 50 Å for J_{11}) of the electrostatic interactions between the transition densities in the intermediate to long distance range, calling into question the validity of the point dipole approximation for an accurate evaluation of the Coulombic couplings in LHCs. $J^{C}_{dip\text{-}dip}$ converges to within 4% of J^{C}_{TDC} at 100 Å, while at a larger distance the two methods diverge since the summation in eq 1 over a large number of grid points of the TDC becomes more prone to accumulation of numerical errors.

Finally, using the same symmetric model system we assessed the relative accuracy of the Coulombic coupling J^{C} (eq 1) by comparing it to the total coupling J^{TOT} obtained from the diabatization procedure. At short distances, the short-range component $J^{short} = J^{TOT} - J^{C}$ follows an overlap-dependent exponential attenuation as shown in the bottom panel of Figure 2, in agreement with ref 29. At long distances, although the interaction is expected to be purely Coulombic, we found a residual deviation between J^{TOT} and J^{C} (3% for J_{11}, 13% for J_{22}, 11% for $J_{12} = J_{21}$), which is nearly constant between 20 and 50 Å. The discrepancy can be attributed to an intrinsic difference between the two approaches. The coupling J^{C} is computed perturbatively between two reference unperturbed wave functions, while J^{TOT} is extracted from the variational solution of the dimer, which includes the relaxation of the orbitals and all the excited state CI coefficients. For this reason, and considering the uncertainty on J^{C} due to the DFT functional, the discrepancy between J^{TOT} and J^{C} can be interpreted more safely as a short-range interaction only when it exceeds 10−15%.

Short-Range Interactions in Light Harvesting Complexes. The spatial arrangements of the chromophores are more heterogeneous in LHCs than in molecular materials (see Figure 1), with a few closely spaced chromophore pairs interacting much more strongly than the others. In Figure 3 we compare J^{TOT} and J^{C} separately for the three light harvesting complexes. Different symbols are used for different pairs of identical chromophores. When close and distant pairs are present, we have separated the data for chromophore pairs within a minimum intermolecular distance D = 7 Å from the more distant ones. For pairs not in close contact (D > 7 Å), we observe that the couplings are in general smaller than 10 meV, showing root-mean-square deviation (RMSD) between J^{C} and $|J^{TOT}|$ smaller than 1 meV, and RMS relative error of ∼12%. In other words, in pairs separated by long distances the deviations do not significantly exceed the uncertainty attributable to different computational methods, and the excitonic couplings are described reasonably well by the Coulombic interaction. Conversely, the chromophore pairs with short distance contacts (D < 7 Å) have significantly larger RMSD (by 1 order of magnitude), and in a few pairs the short-range components represent a substantial fraction of the total coupling. The couplings with the largest short-range contributions are reported in Table 1. These chromophore pairs are strongly coupled due to significant intermolecular overlap, such as the neighboring BChlA in the B850 ring of LH2, a few BChlA pairs in FMO, and peridinin pairs in PCP (see also Figure 1). The values of J^{TOT} and J^{short} for dimers A and B in LH2 obtained by Scholes and co-workers[40] are reported in Table 1 for comparison. The differences are mainly due to the well-known overestimation of $|\boldsymbol{\mu}|$ by the CIS method (see ref 40 and references therein), which results in a factor of ∼2 overestimation of the splitting between the two lowest excited states in the dimer compared to our TDDFT calculation. The resulting J^{TOT} and J^{C} couplings obtained by Scholes et al. are therefore overestimated by a factor of ∼2, but the short-range component is found to be of similar relative importance. It is also worth noting that in FMO and LH2 some of the strongest short-range interactions are those which enhance the otherwise rather weak J_{22}, J_{12}, and J_{21} Coulombic couplings. If one limits the analysis to the J_{11} couplings,[8,9] the Coulombic interaction may offer a sufficiently accurate description of the excitonic couplings, but this is not necessarily the case if the couplings involving S_2 have to be included in the exciton dynamics, as discussed in the Methods section. It was verified that including S_2 of BChlA in the diabatization procedure does not significantly affect the J_{11} couplings. The RMSD between the J_{11} couplings obtained without and with S_2 was found to be 0.056 meV in FMO and 0.010 meV in LH2. These results have two major implications to consider when studying the excitonic properties of LHCs. First, short-range effects need to be included when studying their exciton dynamics, since the

DOI: 10.1021/acs.jctc.7b00328
J. Chem. Theory Comput. 2017, 13, 3754−3763

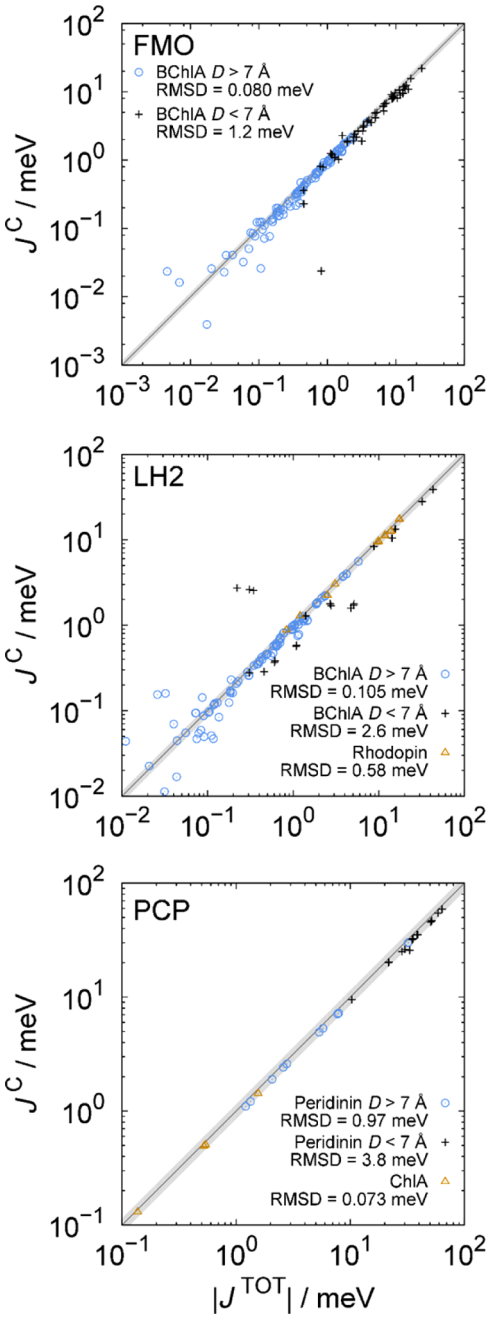

Figure 3. Coulombic couplings (from TDCs) plotted against total excitonic couplings between chromophore pairs in LHCs. The shaded area corresponds to a ±15% deviation from the $J^{C} = |J^{TOT}|$ line.

properties of the excitonic Hamiltonian are determined by the strongest couplings between closely spaced chromophores rather than by the average couplings. Moreover, including the second excited state and computing the cross-couplings may be crucial for a complete and accurate description of these systems.

Short-Range Interactions in Molecular Semiconductors. We will now examine the role short-range interactions in the molecular solids considered. In the disordered ZnPc model we consider separately a set of 10 intercolumn dimers and 90 intracolumn dimers (first neighbors), reported in the top and bottom panels of Figure 4, respectively. The interactions between molecules in adjacent columns in ZnPc are characterized by moderate couplings in the 1−30 meV range, and small short-range contributions are easily rationalized in

Table 1. Couplings with the Largest Short-Range Contributions J^{short} for Each of the LHCs[b]

system	pair	D/Å	coupled states	J^{TOT}	$J^{short}\left(\frac{J^{short}}{J^{TOT}}\right)$
FMO	1-2	2.26	1,2	15.2	4.29 (28%)
	5-6	2.61	1,2	12.6	3.19 (25%)
	5-6	2.61	2,1	13.6	2.61 (19%)
	4-7	2.58	1,2	11.5	2.59 (22%)
	3-7	2.18	1,2	10.5	2.41 (23%)
LH2	A[a]		1,1	90.5	6.8 (7.5%)
	B[a]		1,1	68.2	7.4 (11%)
	A	1.90	1,1	42.9	4.31 (10%)
	B	1.71	1,1	32.0	4.12 (13%)
	A	1.90	2,2	14.3	3.82 (27%)
	A	1.90	1,2	4.98	3.30 (66%)
	B	1.71	2,2	15.5	2.24 (14%)
PCP	4-7	0.98	1,1	33.1	7.41 (22%)
	1-3	2.53	1,1	50.7	5.16 (10%)
	7-8	2.65	1,1	51.8	5.08 (10%)
	2-4	2.40	1,1	63.6	4.50 (7.1%)
	5-6	2.98	1,1	58.7	4.24 (7.2%)

[a]Results are from ref 40. [b]All couplings are in meV. In LH2 each value is averaged over all equivalent pairs (three of type A and two of type B in the B850 ring as indicated in Figure 1).

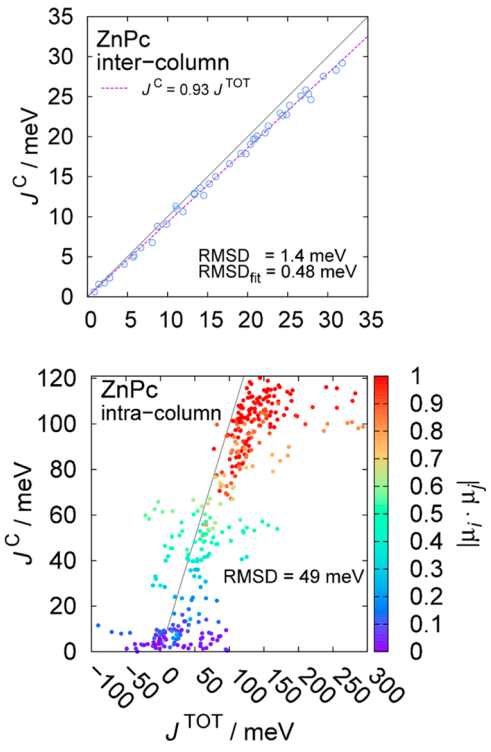

Figure 4. Coulombic couplings (from TDCs) plotted against total excitonic couplings in disordered ZnPc. Top: the dashed line is a linear fit to the data points. Bottom: neighboring intracolumn dimers. The color of the data points is proportional to the absolute value of the dot product between the transition dipole moments of the localized excitations.

terms of a very small intermolecular overlap. This results in a small systematic shift corresponding to a relative short-range contribution $J^{short}/J^{TOT} = 7.5\%$ as quantified by a linear fit to the data (see the top panel of Figure 4). As this does not significantly exceed the deviation due to the methods, we

DOI: 10.1021/acs.jctc.7b00328
J. Chem. Theory Comput. 2017, 13, 3754−3763

conclude that for intercolumn dimers J^C is a good approximation of J^{TOT}. On the other hand, in the intracolumn dimers, where there is significant orbital overlap between molecules, the excitonic couplings are dominated by the short-range interactions J^{short}, which are found to be very large: up to 195 meV (66% of J^{TOT}). The set of couplings in this disordered sample has very peculiar characteristics, as is evident in the bottom panel of Figure 4. For J^C smaller than 70 meV, occurring when the transition dipoles are not well-aligned, the sign of J^{short} is not correlated with J^C, i.e. the short-range effects can either enhance or diminish $|J^{TOT}|$ with respect to J^C. Surprisingly, when J^C is larger than 70 meV, J^{short} always has the same sign as J^C, resulting in J^{TOT} always being stronger than J^C. In the range of couplings found in this system, where the strongest J^C is around 100 meV but J^{TOT} can be as high as 290 meV, a correct consideration of the short-range interactions may make the difference between incoherent (or intermediate) and coherent exciton transport regime since the reorganization energy of ZnPc is ∼40 meV.[81]

Further insight into the role of short-range interactions is given by examining the couplings between neighboring molecules in the OBPc crystal subject to thermal fluctuations. The spectroscopy and exciton dynamics of this system are mainly determined by the couplings in the intracolumn dimers A and B.[36,53] The very short $\pi-\pi$ intermolecular distances in the 3.5−4.5 Å range (see Figure 1) make these couplings very sensitive to thermal fluctuations. The values of J^C and J^{TOT} for 250 MD snapshots are shown in Figure 5. We first note that the short-range contributions J^{short} can make up a significant fraction (up to 60%) of J^{TOT} and, in this case, can also influence the regime of exciton transport since the reorganization energy was found to be of the same order of magnitude (∼100 meV).[36] Furthermore, for all couplings the distributions of J^{TOT} are significantly wider than those of J^C, confirming the primary role of short-range effects in determining the thermal fluctuations of the couplings. Finally, as is evident from Figure 5, the short-range component in dimer A tends to have the same sign as the Coulombic coupling, while in dimer B there appears to be no correlation at all. This striking difference between the apparently similar dimers A and B can be intuitively rationalized in terms of overlap: dimer A has a prevalently face-to-face arrangement with overlap extending over more than half of the molecular surface, while dimer B has a head-to-tail character with only one of the isoindole units overlapping (see the right panel of Figure 5). In general, one would not expect to observe such a strong correlation between the signs of Coulombic and short-range interactions.[2] However, in some specific cases with large intermolecular overlap, such as dimer A of OBPc or the most strongly coupled intracolumn dimers of ZnPc, the short-range interaction can be strongly correlated with the Coulombic interaction, systematically reinforcing it when it is already strong. Conversely when the overlap is smaller, e.g. in head-to-tail configurations such as dimer B of OBPc, the short-range component can still be large in magnitude, but the sign is not necessarily correlated with that of the Coulombic interaction. It should be noted that a similar correlation was reported for the naphthalene dimer by Scholes and Ghiggino.[29] Since this correlation effect depends on the specific wave functions and packing geometry of a given system, its occurrence may be difficult to predict without actually computing the couplings.

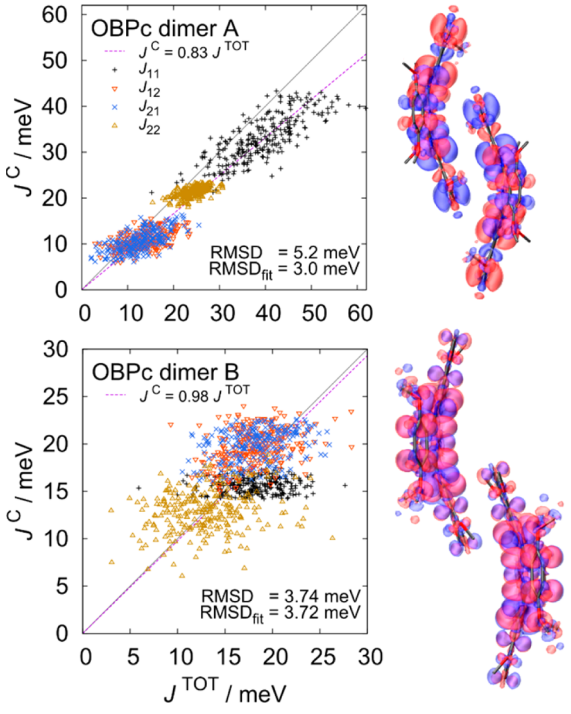

Figure 5. Left: Coulombic couplings (from TDCs) plotted against the total excitonic couplings in two dimers of the OBPc molecular crystal, computed along a MD simulation (250 snapshots every 50 fs) described in ref 36. The dashed lines are linear fits to the data points. Right: Transition density plots (generated with VMD[57]) of the S_1 excited state localized on the molecules in the two dimers at the crystal geometry.

CONCLUSIONS

The importance of short-range effects on excitonic couplings between chromophores in three natural light harvesting complexes and two organic semiconductors has been investigated, comparing the total excitonic coupling (computed via a diabatization scheme) and the Coulombic component (using a fine grid representation of the transition density). For molecules not in close contact, as expected, the Coulombic coupling is comparable to the coupling obtained by diabatization. The discrepancies are typically of around 10%, i.e. below what can be considered important for the description of excitonic physics also considering the variability among computational methods.

When the interacting molecules are in close contact, the stronger couplings can be significantly affected by short-range effects. Among the natural LHCs studied, only a few pairs of chromophores are strongly coupled. In FMO, the most strongly coupled dimers have short-range components up to ∼4 meV (28% of the total coupling). The neighboring BChlA chromophores in the B850 ring of LH2 also exhibit significant short-range interactions up to ∼4 meV and up to 66% of the total coupling (∼3 meV out of ∼5 meV). In PCP, only two of the peridinin dimers have moderate short-range components of ∼7 and ∼5 meV (22% and 10% of the total coupling). Although in general the couplings between chromophores are well described by the Coulombic interaction, the excitonic properties of the aggregates are expected to be dominated by the strongest couplings, i.e. those between neighboring chromophores which require the evaluation of short-range contributions.

DOI: 10.1021/acs.jctc.7b00328
J. Chem. Theory Comput. 2017, 13, 3754−3763

In molecular solids, the excitonic coupling in closely packed face-to-face dimers is dominated by short-range interactions which are found to be very large: up to 200 meV (70% of the total coupling). For the particular materials considered in this work we found that when the Coulombic coupling is stronger than 70 meV, the short-range component always has the same sign as the Coulombic coupling, making the total coupling even stronger when it is already large. This effect of reinforcement, which is found to be present in face-to-face but not in head-to-tail dimers, is potentially very important for the mechanism of exciton diffusion as stronger coupling favors more coherent dynamics.

■ ASSOCIATED CONTENT

Supporting Information

The Supporting Information is available free of charge on the ACS Publications website at DOI: 10.1021/acs.jctc.7b00328.

Structures (.xyz format) of all the molecular dimers for which the coupling was computed (ZIP)

■ AUTHOR INFORMATION

Corresponding Author

*E-mail: a.troisi@liverpool.ac.uk.

ORCID

Patrick Rowe: 0000-0003-3897-9181

Alessandro Troisi: 0000-0002-5447-5648

Present Address

§Department of Physics and Astronomy, University College London, London, WC1E 6BT, United Kingdom.

Funding

This work is supported by the European Research Council (Grant No. 615834).

Notes

The authors declare no competing financial interest.

■ REFERENCES

(1) Curutchet, C.; Mennucci, B. Quantum Chemical Studies of Light Harvesting. *Chem. Rev.* **2017**, *117*, 294−343.

(2) Mirkovic, T.; Ostroumov, E. E.; Anna, J. M.; van Grondelle, R.; Govindjee; Scholes, G. D. Light Absorption and Energy Transfer in the Antenna Complexes of Photosynthetic Organisms. *Chem. Rev.* **2017**, *117*, 249−293.

(3) Stangl, T.; Wilhelm, P.; Schmitz, D.; Remmerssen, K.; Henzel, S.; Jester, S. S.; Höger, S.; Vogelsang, J.; Lupton, J. M. Temporal Fluctuations in Excimer-like Interactions between π-Conjugated Chromophores. *J. Phys. Chem. Lett.* **2015**, *6*, 1321−1326.

(4) Scholes, G. D.; Rumbles, G. Excitons in Nanoscale Systems. *Nat. Mater.* **2006**, *5*, 683−696.

(5) Tant, J.; Geerts, Y. H.; Lehmann, M.; De Cupere, V.; Zucchi, G.; Laursen, B. W.; Bjørnholm, T.; Lemaur, V.; Marcq, V.; Burquel, A.; Hennebicq, E.; Gardebien, F.; Viville, P.; Beljonne, D.; Lazzaroni, R.; Cornil, J. Liquid Crystalline Metal-Free Phthalocyanines Designed for Charge and Exciton Transport. *J. Phys. Chem. B* **2005**, *109*, 20315−20323.

(6) Olbrich, C.; Jansen, T. L. C.; Liebers, J.; Aghtar, M.; Strümpfer, J.; Schulten, K.; Knoester, J.; Kleinekathöfer, U. From Atomistic Modeling to Excitation Transfer and Two-Dimensional Spectra of the FMO Light-Harvesting Complex. *J. Phys. Chem. B* **2011**, *115*, 8609−8621.

(7) Shim, S.; Rebentrost, P.; Valleau, S.; Aspuru-Guzik, A. Atomistic Study of the Long-Lived Quantum Coherences in the Fenna-Matthews-Olson Complex. *Biophys. J.* **2012**, *102*, 649−660.

(8) Jurinovich, S.; Curutchet, C.; Mennucci, B. The Fenna-Matthews-Olson Protein Revisited: A Fully Polarizable (TD)DFT/MM Description. *ChemPhysChem* **2014**, *15*, 3194−3204.

(9) Cupellini, L.; Jurinovich, S.; Campetella, M.; Caprasecca, S.; Guido, C. A.; Kelly, S. M.; Gardiner, A. T.; Cogdell, R.; Mennucci, B. An Ab Initio Description of the Excitonic Properties of LH2 and Their Temperature Dependence. *J. Phys. Chem. B* **2016**, *120*, 11348−11359.

(10) Aghtar, M.; Kleinekathöfer, U.; Curutchet, C.; Mennucci, B. Impact of Electronic Fluctuations and Their Description on the Exciton Dynamics in the Light-Harvesting Complex PE545. *J. Phys. Chem. B* **2017**, *121*, 1330−1339.

(11) Haverkort, F.; Stradomska, A.; de Vries, A. H.; Knoester, J. First-Principles Calculation of the Optical Properties of an Amphiphilic Cyanine Dye Aggregate. *J. Phys. Chem. A* **2014**, *118*, 1012−1023.

(12) van der Vegte, C. P.; Prajapati, J. D.; Kleinekathöfer, U.; Knoester, J.; Jansen, T. L. C. Atomistic Modeling of Two-Dimensional Electronic Spectra and Excited-State Dynamics for a Light Harvesting 2 Complex. *J. Phys. Chem. B* **2015**, *119*, 1302−1313.

(13) Aragó, J.; Troisi, A. Dynamics of the Excitonic Coupling in Organic Crystals. *Phys. Rev. Lett.* **2015**, *114*, 26402.

(14) Durrant, J. R.; Knoester, J.; Wiersma, D. A. Local Energetic Disorder in Molecular Aggregates Probed by the One-Exciton to Two-Exciton Transition. *Chem. Phys. Lett.* **1994**, *222*, 450−456.

(15) Clark, J.; Silva, C.; Friend, R. H.; Spano, F. C. Role of Intermolecular Coupling in the Photophysics of Disordered Organic Semiconductors: Aggregate Emission in Regioregular Polythiophene. *Phys. Rev. Lett.* **2007**, *98*, 1−10.

(16) Dykstra, T. E.; Hennebicq, E.; Beljonne, D.; Gierschner, J.; Claudio, G.; Bittner, E. R.; Knoester, J.; Scholes, G. D. Conformational Disorder and Ultrafast Exciton Relaxation in PPV-Family Conjugated Polymers. *J. Phys. Chem. B* **2009**, *113*, 656−667.

(17) Barford, W.; Trembath, D. Exciton Localization in Polymers with Static Disorder. *Phys. Rev. B: Condens. Matter Mater. Phys.* **2009**, *80*, 165418.

(18) Zhang, X.; Li, Z.; Lu, G. First-Principles Simulations of Exciton Diffusion in Organic Semiconductors. *Phys. Rev. B: Condens. Matter Mater. Phys.* **2011**, *84*, 235208.

(19) Saikin, S. K.; Eisfeld, A.; Valleau, S.; Aspuru-Guzik, A. Photonics Meets Excitonics: Natural and Artificial Molecular Aggregates. *Nanophotonics* **2013**, *2*, 21−38.

(20) Tapping, P. C.; Clafton, S. N.; Schwarz, K. N.; Kee, T. W.; Huang, D. M. Molecular-Level Details of Morphology-Dependent Exciton Migration in Poly(3-Hexylthiophene) Nanostructures. *J. Phys. Chem. C* **2015**, *119*, 7047−7059.

(21) Hsu, C.; You, Z.; Chen, H. Characterization of the Short-Range Couplings in Excitation Energy Transfer. *J. Phys. Chem. C* **2008**, *112*, 1204−1212.

(22) McWeeny, R. *Methods of Molecular Quantum Mechanics*, 2nd ed.; Academic Press: London, 1992.

(23) Krueger, B. P.; Scholes, G. D.; Fleming, G. R. Calculation of Couplings and Energy-Transfer Pathways between the Pigments of LH2 by the Ab Initio Transition Density Cube Method. *J. Phys. Chem. B* **1998**, *102*, 5378−5386.

(24) Hsu, C. The Electronic Couplings in Electron Transfer and Excitation Energy Transfer. *Acc. Chem. Res.* **2009**, *42*, 509−518.

(25) Chang, J. C. Monopole Effects on Electronic Excitation Interactions between Large Molecules. I. Application to Energy Transfer in Chlorophylls. *J. Chem. Phys.* **1977**, *67*, 3901−3909.

(26) Yamagata, H.; Norton, J.; Hontz, E.; Olivier, Y.; Beljonne, D.; Brédas, J.; Silbey, R. J.; Spano, F. C. The Nature of Singlet Excitons in Oligoacene Molecular Crystals. *J. Chem. Phys.* **2011**, *134*, 204703.

(27) Förster, T. Zwischenmolekulare Energiewanderung Und Fluoreszenz. *Ann. Phys.* **1948**, *437*, 55−75.

(28) Harcourt, R. D.; Scholes, G. D.; Ghiggino, K. P. Rate Expressions for Excitation Transfer. II. Electronic Considerations of Direct and Through−configuration Exciton Resonance Interactions. *J. Chem. Phys.* **1994**, *101*, 10521.

(29) Scholes, G. D.; Ghiggino, K. P. Electronic Interactions and Interchromophore Excitation Transfer. *J. Phys. Chem.* **1994**, *98*, 4580−4590.
(30) Scholes, G. D.; Harcourt, R. D.; Ghiggino, K. P. Rate Expressions for Excitation Transfer. III. An Ab Initio Study of Electronic Factors in Excitation Transfer and Exciton Resonance Interactions. *J. Chem. Phys.* **1995**, *102*, 9574.
(31) Cave, R. J.; Newton, M. D. Generalization of the Mulliken-Hush Treatment for the Calculation of Electron Transfer Matrix Elements. *Chem. Phys. Lett.* **1996**, *249*, 15−19.
(32) Voityuk, A. A. Estimation of Electronic Coupling for Singlet Excitation Energy Transfer. *J. Phys. Chem. C* **2014**, *118*, 1478−1483.
(33) Hoyer, C. E.; Xu, X.; Ma, D.; Gagliardi, L.; Truhlar, D. G. Diabatization Based on the Dipole and Quadrupole: The DQ Method. *J. Chem. Phys.* **2014**, *141*, 114104.
(34) Aragó, J.; Troisi, A. Excitonic Couplings between Molecular Crystal Pairs by a Multistate Approximation. *J. Chem. Phys.* **2015**, *142*, 164107.
(35) May, V.; Kühn, O. *Charge and Energy Transfer Dynamics in Molecular Systems*, 3rd ed.; Wiley-VCH: Weinheim, Germany, 2011.
(36) Fornari, R. P.; Aragó, J.; Troisi, A. Exciton Dynamics in Phthalocyanine Molecular Crystals. *J. Phys. Chem. C* **2016**, *120*, 7987−7996.
(37) Aragó, J.; Troisi, A. Regimes of Exciton Transport in Molecular Crystals in the Presence of Dynamic Disorder. *Adv. Funct. Mater.* **2016**, *26*, 2316−2325.
(38) Vlaming, S. M.; Silbey, R. J. Correlated Intermolecular Coupling Fluctuations in Photosynthetic Complexes. *J. Chem. Phys.* **2012**, *136*, 055102.
(39) Huo, P.; Coker, D. F. Influence of Environment Induced Correlated Fluctuations in Electronic Coupling on Coherent Excitation Energy Transfer Dynamics in Model Photosynthetic Systems. *J. Chem. Phys.* **2012**, *136*, 115102.
(40) Scholes, G. D.; Gould, I. R.; Cogdell, R. J.; Fleming, G. R. Ab Initio Molecular Orbital Calculations of Electronic Couplings in the LH2 Bacterial Light-Harvesting Complex of Rps-Acidophila. *J. Phys. Chem. B* **1999**, *103*, 2543−2553.
(41) Engel, G. S.; Calhoun, T. R.; Read, E. L.; Ahn, T.-K.; Mancal, T.; Cheng, Y.-C.; Blankenship, R. E.; Fleming, G. R. Evidence for Wavelike Energy Transfer through Quantum Coherence in Photosynthetic Systems. *Nature* **2007**, *446*, 782−786.
(42) Hildner, R.; Brinks, D.; Nieder, J. B.; Cogdell, R. J.; van Hulst, N. F. Quantum Coherent Energy Transfer over Varying Pathways in Single Light-Harvesting Complexes. *Science* **2013**, *340*, 1448−1451.
(43) Chenu, A.; Scholes, G. D. Coherence in Energy Transfer and Photosynthesis. *Annu. Rev. Phys. Chem.* **2015**, *66*, 69−96.
(44) Kim, H. W.; Kelly, A.; Park, J. W.; Rhee, Y. M. All-Atom Semiclassical Dynamics Study of Quantum Coherence in Photosynthetic Fenna − Matthews − Olson Complex. *J. Am. Chem. Soc.* **2012**, *134*, 11640−11651.
(45) Lee, M. H.; Troisi, A. Vibronic Enhancement of Excitation Energy Transport: Interplay between Local and Non-Local Exciton-Phonon Interactions. *J. Chem. Phys.* **2017**, *146*, 075101.
(46) Olson, J. M. The FMO Protein. In *Discoveries in Photosynthesis*; Govindjee, Beatty, J. T., Gest, H., Allen, J. F., Eds.; Springer: Dordrecht, The Netherlands, 2005; pp 421−427.
(47) McDermott, G.; Prince, S. M.; Freer, A. A.; Hawthornthwaite-Lawless, A. M.; Papiz, M. Z.; Cogdell, R. J.; Isaacs, N. W. Crystal Structure of an Integral Membrane Light-Harvesting Complex from Photosynthetic Bacteria. *Nature* **1995**, *374*, 517−521.
(48) Hofmann, E.; Wrench, P. M.; Sharples, F. P.; Hiller, R. G.; Welte, W.; Diederichs, K. Structural Basis of Light Harvesting by Carotenoids: Peridinin-Chlorophyll-Protein from Amphidinium Carterae. *Science* **1996**, *272*, 1788.
(49) Ishizaki, A.; Fleming, G. R. Theoretical Examination of Quantum Coherence in a Photosynthetic System at Physiological Temperature. *Proc. Natl. Acad. Sci. U. S. A.* **2009**, *106*, 17255−17260.
(50) Cogdell, R. J.; Gall, A.; Köhler, J. The Architecture and Function of the Light-Harvesting Apparatus of Purple Bacteria: From Single Molecules to in Vivo Membranes. *Q. Rev. Biophys.* **2006**, *39*, 227.
(51) Jimenez, R.; Dikshit, S. N.; Bradforth, S. E.; Fleming, G. R. Electronic Excitation Transfer in the LH2 Complex of Rhodobacter Sphaeroides. *J. Phys. Chem.* **1996**, *100*, 6825−6834.
(52) Bricker, W. P.; Lo, C. S. Efficient Pathways of Excitation Energy Transfer from Delocalized S2 Excitons in the Peridinin−Chlorophyll a − Protein Complex. *J. Phys. Chem. B* **2015**, *119*, 5755−5764.
(53) Rawat, N.; Pan, Z.; Manning, L. W.; Lamarche, C. J.; Cour, I.; Headrick, R. L.; Waterman, R.; Woll, A. R.; Furis, M. I. Macroscopic Molecular Ordering and Exciton Delocalization in Crystalline Phthalocyanine Thin Films. *J. Phys. Chem. Lett.* **2015**, *6*, 1834−1840.
(54) Wo, S.; Headrick, R. L.; Anthony, J. E. Fabrication and Characterization of Controllable Grain Boundary Arrays in Solution-Processed Small Molecule Organic Semiconductor Films. *J. Appl. Phys.* **2012**, *111*, 073716.
(55) Rivnay, J.; Mannsfeld, S. C. B.; Miller, C. E.; Salleo, A.; Toney, M. F. Quantitative Determination of Organic Semiconductor Microstructure from the Molecular to Device Scale with Quantitative X-Ray Scattering and Absorption Analyses. *Chem. Rev.* **2012**, *112*, 5488−5519.
(56) Pan, Z.; Rawat, N.; Cour, I.; Manning, L.; Headrick, R. L.; Furis, M. Polarization-Resolved Spectroscopy Imaging of Grain Boundaries and Optical Excitations in Crystalline Organic Thin Films. *Nat. Commun.* **2015**, *6*, 8201.
(57) Humphrey, W.; Dalke, A.; Schulten, K. VMD: Visual Molecular Dynamics. *J. Mol. Graphics* **1996**, *14*, 33−38.
(58) Ben-Shem, A.; Frolow, F.; Nelson, N. Evolution of Photosystem I - from Symmetry through Pseudosymmetry to Asymmetry. *FEBS Lett.* **2004**, *564*, 274−280.
(59) Papiz, M. Z.; Prince, S. M.; Howard, T.; Cogdell, R. J.; Isaacs, N. W. The Structure and Thermal Motion of the B800−850 LH2 Complex from Rps. Acidophila at 2.0 Å Resolution and 100 K: New Structural Features and Functionally Relevant Motions. *J. Mol. Biol.* **2003**, *326*, 1523−1538.
(60) Kenny, E. P.; Kassal, I. Benchmarking Calculations of Excitonic Couplings between Bacteriochlorophylls. *J. Phys. Chem. B* **2016**, *120*, 25−32.
(61) Abraham, M. J.; Murtola, T.; Schulz, R.; Páll, S.; Smith, J. C.; Hess, B.; Lindahl, E. Gromacs: High Performance Molecular Simulations through Multi-Level Parallelism from Laptops to Supercomputers. *SoftwareX* **2015**, *1−2*, 19−25.
(62) Dwyer, P. J.; Vander Valk, R. J.; Caltaldo, V.; Demianicz, D.; Kelty, S. P. All-Atom CHARMM Force Field and Bulk Properties of Perfluorozinc Phthalocyanines. *J. Phys. Chem. A* **2014**, *118*, 11583.
(63) Scheidt, W. R.; Dow, W. Molecular Stereochemistry of Phthalocyanatozinc (II). *J. Am. Chem. Soc.* **1977**, *99*, 1101−1104.
(64) Ponder, J. W.; Richards, F. M. An Efficient Newton-like Method for Molecular Mechanics Energy Minimization of Large Molecules. *J. Comput. Chem.* **1987**, *8*, 1016−1024.
(65) Valiev, M.; Bylaska, E. J.; Govind, N.; Kowalski, K.; Straatsma, T. P.; Van Dam, H. J. J.; Wang, D.; Nieplocha, J.; Apra, E.; Windus, T. L.; de Jong, W. A. NWChem: A Comprehensive and Scalable Open-Source Solution for Large Scale Molecular Simulations. *Comput. Phys. Commun.* **2010**, *181*, 1477−1489.
(66) Vydrov, O. A.; Scuseria, G. E. Assessment of a Long-Range Corrected Hybrid Functional. *J. Chem. Phys.* **2006**, *125*, 234109.
(67) Rohrdanz, M. A.; Martins, K. M.; Herbert, J. M. A Long-Range-Corrected Density Functional That Performs Well for Both Ground-State Properties and Time-Dependent Density Functional Theory Excitation Energies, Including Charge-Transfer Excited States. *J. Chem. Phys.* **2009**, *130*, 054112.
(68) Olaya-Castro, A.; Scholes, G. D. Energy Transfer from Förster−Dexter Theory to Quantum Coherent Light- Harvesting. *Int. Rev. Phys. Chem.* **2011**, *30*, 49−77.
(69) Krueger, B. P.; Scholes, G. D.; Jimenez, R.; Fleming, G. R. Electronic Excitation Transfer from Carotenoid to Bacteriochlorophyll

DOI: 10.1021/acs.jctc.7b00328
J. Chem. Theory Comput. 2017, 13, 3754−3763

in the Purple Bacterium Rhodopseudomonas Acidophila. *J. Phys. Chem. B* **1998**, *102*, 2284−2292.
(70) Tretiak, S.; Middleton, C.; Chernyak, V.; Mukamel, S. Bacteriochlorophyll and Carotenoid Excitonic Couplings in the LH2 System of Purple Bacteria. *J. Phys. Chem. B* **2000**, *104*, 9540−9553.
(71) Wan, Y.; Stradomska, A.; Fong, S.; Guo, Z.; Schaller, R. D.; Wiederrecht, G. P.; Knoester, J.; Huang, L. Exciton Level Structure and Dynamics in Tubular Porphyrin Aggregates. *J. Phys. Chem. C* **2014**, *118*, 24854−24865.
(72) Kiss, P. T.; Sega, M.; Baranyai, A. Efficient Handling of Gaussian Charge Distributions: An Application to Polarizable Molecular Models. *J. Chem. Theory Comput.* **2014**, *10*, 5513−5519.
(73) Curutchet, C.; Kongsted, J.; Muñoz-Losa, A.; Hossein-Nejad, H.; Scholes, G. D.; Mennucci, B. Photosynthetic Light-Harvesting Is Tuned by the Heterogeneous Polarizable Environment of the Protein. *J. Am. Chem. Soc.* **2011**, *133*, 3078−3084.
(74) Mennucci, B.; Curutchet, C. The Role of the Environment in Electronic Energy Transfer: A Molecular Modeling Perspective. *Phys. Chem. Chem. Phys.* **2011**, *13*, 11538−11550.
(75) Rosnik, A. M.; Curutchet, C. Theoretical Characterization of the Spectral Density of the Water-Soluble Chlorophyll-Binding Protein from Combined Quantum Mechanics/Molecular Mechanics Molecular Dynamics Simulations. *J. Chem. Theory Comput.* **2015**, *11*, 5826−5837.
(76) Padula, D.; Jurinovich, S.; Di Bari, L.; Mennucci, B. Simulation of Electronic Circular Dichroism of Nucleic Acids: From the Structure to the Spectrum. *Chem. - Eur. J.* **2016**, *22*, 17011−17019.
(77) Adolphs, J.; Müh, F.; Madjet, M. E. A.; Renger, T. Calculation of Pigment Transition Energies in the FMO Protein: From Simplicity to Complexity and Back. *Photosynth. Res.* **2008**, *95*, 197−209.
(78) Renger, T.; Müh, F. Understanding Photosynthetic Light-Harvesting: A Bottom up Theoretical Approach. *Phys. Chem. Chem. Phys.* **2013**, *15*, 3348−3371.
(79) Kistler, K. A.; Spano, F. C.; Matsika, S. A Benchmark of Excitonic Couplings Derived from Atomic Transition Charges. *J. Phys. Chem. B* **2013**, *117*, 2032−2044.
(80) Madjet, M. E.; Abdurahman, A.; Renger, T. Intermolecular Coulomb Couplings from Ab Initio Electrostatic Potentials: Application to Optical Transitions of Strongly Coupled Pigments in Photosynthetic Antennae and Reaction Centers. *J. Phys. Chem. B* **2006**, *110*, 17268−17281.
(81) da Silva Filho, D. a; Coropceanu, V.; Gruhn, N. E.; de Oliveira Neto, P. H.; Brédas, J.-L. Intramolecular Reorganization Energy in Zinc Phthalocyanine and Its Fluorinated Derivatives: A Joint Experimental and Theoretical Study. *Chem. Commun.* **2013**, *49*, 6069−6071.

DOI: 10.1021/acs.jctc.7b00328
J. Chem. Theory Comput. 2017, 13, 3754−3763